Journal of Geodynamics 51 (2011) 339–343

Contents lists available at ScienceDirect

Journal of Geodynamics

journal homepage: http://www.elsevier.com/locate/jog

Determining and modeling tectonic movements along the central part of the North Anatolian Fault (Turkey) using geodetic measurements

Hakan Yavaşoğlu[a,*], Ergin Tarı[a], Okan Tüysüz[b], Ziyadin Çakır[c], Semih Ergintav[d]

[a] ITU Geomatics Eng., 34469, Maslak, Istanbul, Turkey
[b] ITU Eurasia Earth Science Institute, Istanbul, Turkey
[c] ITU Geological Engineering, Istanbul, Turkey
[d] TUBITAK, Marmara Research Center, Kocaeli, Turkey

ARTICLE INFO

Article history:
Received 25 November 2009
Received in revised form 23 July 2010
Accepted 24 July 2010
Available online 5 August 2010

Keywords:
Active tectonics
North Anatolian Fault
Slip rate
GPS
Turkey

ABSTRACT

The North Anatolian Fault (NAF), which extends from Karlıova in Eastern Turkey to the Gulf of Saros in the Northern Aegean Sea, is one of the longest active strike-slip faults in the world with a length of about 1500 km. Within the North Anatolian Shear Zone (NASZ) there are long splays off the main trunk of the NAF veering towards the interior parts of Anatolia. Although the whole shear zone is still seismically active, the major seismicity is concentrated along the main branch of the NAF. Splays of the NAF dissect the shear zone into different continental blocks. The largest splay of the NAF was selected to analyze the distribution of movements between the faults delimiting these blocks. Four years of GPS measurements and modeling results indicate that the differential motion between the Anatolian collage and the Eurasian plate along the central part of the NAF is partitioned between fault splays and varies between 18.7 ± 1.6 and 21.5 ± 2.1 mm/yr with the main branch taking ~90% of the motion.

1. Introduction

Following the collision of the Arabian and Anatolian plates in Southeastern Turkey (Şengör and Yılmaz, 1981), the Anatolian plate started to escape westward about 5 Ma ago along two strike-slip faults; the Northern and the Eastern Anatolian Transform faults (NAF and EAZ, respectively). The NAF is only a member of a large dextral shear zone, the North Anatolian Shear Zone (NASZ), reaching up to 100 km in width (Şengör et al., 2004). Within the NASZ, there are different offshoots (splays) that bifurcate from the main branch of the NAF and extend into the interior parts of Anatolia. Both the main branch and the offshoots divide the shear zone into fault-bounded blocks. As a result of differential movements along both the main branch and the offshoots, these fault-delimited blocks display different rotations as indicated by palaeomagnetic studies (Platzman et al., 1994, 1998; Tatar et al., 1995, 1996; Piper et al., 1997; Kaymakçı et al., 2003, 2007; İşseven and Tüysüz, 2006; Avşar and İşseven, 2009). In this paper, we focused on the largest offshoot, the Sungurlu fault, to analyze the partitioning of movements between blocks in NASZ using the GPS technique.

The main branch of the NAF forms the northern boundary of the westward moving Anatolian accretionary collage (Fig. 1). In the study area, the 1943 Tosya earthquake ($M = 7.6$) occurred on the main branch which produced a 260 km surface rupture and right lateral offsets reaching up to 4.5 m (Barka, 1996). The Sungurlu fault leaves the main trunk around the town of Niksar to the east and extends southwestwards. The eastern part of the Sungurlu fault was displaced during the 1939 Erzincan earthquake with a surface rupture 370 km in length ($M = 7.9$, Barka, 1992, 1996). The Çaldağ, Osmancık, Gümüş, Merzifon and Amasya blocks are located between the Sungurlu fault and the main branch of the NAF and are separated from each other by secondary faults (Fig. 1). These are also active as indicated by historical and instrumental earthquake records (Eyidoğan et al., 1991; Ambraseys and Finkel, 1995).

2. The GPS data

2.1. The GPS measurements

The Central NAF GPS network (MID-NAF) was designed to control the movements of both the main branch of the NAF and the block-bounding active faults published in several studies (Piper et al., 1996; Kaymakçı et al., 2001, 2003; İşseven and Tüysüz, 2006) using 16 force-centered measurement stations (Fig. 1). The GPS measurements were started in August 2001 and repeated during the following four years. Campaigns were realized to sample the same time of the year in order to minimize any seasonal variations. The first campaign was performed in between DOYs 233 and 240,

* Corresponding author. Tel.: +90 2122856653.
E-mail address: yavasoglu@itu.edu.tr (H. Yavaşoğlu).

0264-3707/$ – see front matter
doi:10.1016/j.jog.2010.07.003

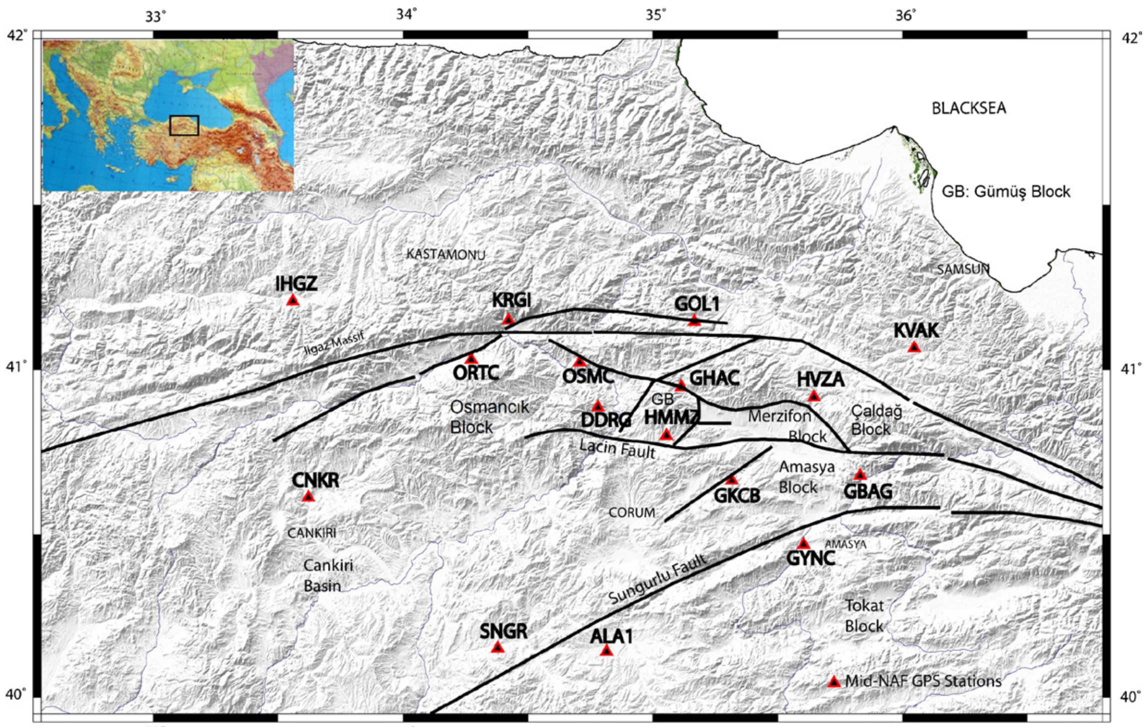

Fig. 1. Shaded topographic image of north central of Turkey showing the main active faults (black lines) (from Okay and Tüysüz, 1999; İşseven and Tüysüz, 2006) and the locations of the GPS sites (triangles).

the second between 217 and 224, the third between 217 and 223, and finally the fourth between 210 and 216. While SNGR (Sungurlu) and IHGZ (İhsangazi) were selected as continuous stations at the first campaign, IHGZ and ALA1 were chosen at the second campaign. During both the third and the fourth campaigns SNGR and IHGZ stations were run throughout the campaign in order to link our measurements together to the International GPS Service for Geodynamics (IGS) network. The duration of the measurements was about 8 h/day with an interval of 30 s and all sites were observed on three consecutive days.

2.2. GPS data analysis

Pseudo-range and phase GPS data are analyzed using GAMIT software as single-day solutions (King and Bock, 2003). Station coordinates, satellite orbits, 13 tropospheric zenith delay parameters per site and phase ambiguities using doubly-differenced phase measurements are solved while applying loose a priori constraints to all parameters.

The IGS final orbits, IERS earth orientation parameters are used, and azimuth and elevation dependent antenna phase center models are applied as recommended by IGS and Tari and King (2002). In addition to our sites and 7 IGS stations in the first campaign and 11 IGS stations in the other campaigns are incorporated into the analyses to serve as ties to ITRF2000 (Table 1).

We determined weights both from IGS and our process solutions, which were combined separately. In addition, repeatability of measured days and their normalized root mean square (nrms) and weighted root mean square (wrms) were used to check accuracy of the measurements. Finally, the reference frame for our velocity estimates was defined by using generalized constraints for transformation parameters (McClusky et al., 2000). The Eurasian plate was defined by minimizing horizontal velocities of sites as given by McClusky et al. (2000) (Table 2). After the transformation, the root mean square (rms) of stations was only 0.5 mm/yr.

Table 1
Global GPS sites used in the analysis.

First campaign		Other campaigns	
Station	Location	Station	Location
ANKR	Ankara, Turkey	ANKR	Ankara, Turkey
BUCU	Bucuresti, Romania	GRAZ	Graz, Austria
ISTA	Istanbul, Turkey	ISTA	Istanbul, Turkey
MATE	Matera, Italy	MATE	Matera, Italy
TELA	Tel Aviv, Israel	MERS	Mersin, Turkey
TUBI	Tubitak, Turkey	TUBI	Tubitak, Turkey
NICO	Nicosia, South Cyprus	ONSA	Onsala, Sweden
		SOFI	Sofia, Bulgaria
		WTZR	Wettzell, Germany
		ZECK	Zelenchukskaya, Russia
		NICO	Nicosia, South Cyprus

Table 2
GPS sites used for definition of Eurasia plate.

Site ID	Location	Site ID	Location
ONSA	Onsala, Sweden	BOR1	Boroweic, Poland
NYAL	Ny-Alesund, Norway	BRUS	Brussels, Belgium
POL2	Bishkek, Kyrghyzstan	HERS	Hailsham, England
POTS	Potsdam, Germany	GRAZ	Graz, Austria
TROM	Tromsoe, Norway	JOZE	Jozefoslaw, Poland
WTZR	Koetzting, Germany	KIT3	Kitab, Uzbekistan
ZIMM	Zimmerwald, Switzerland	KOSG	Kootwijk, The Netherlands
ZWEN	Zwenigorod, Russia	METS	Kirkkonummi, Finland

The results of our analysis are given in Table 3 and Fig. 2 with respect to the Eurasian plate. The RHO in Table 3 is the correlation coefficient between east and north uncertainties.

3. Block model

Previous studies indicate that the crust to the south of the Anatolian Block is escaping westward along the EAF and the NAF

Table 3
GPS site velocities with 1σ uncertainties.

Long (°)	Lat (°)	E Vel (mm/yr)	N Vel (mm/yr)	E $\sigma\pm$ (mm/yr)	N $\sigma\pm$ (mm/yr)	Sites
34.272	41.031	−12.96	3.19	1.09	1.26	ORTC
33.558	41.208	−2.59	1.28	0.66	0.63	IHGZ
33.620	40.614	−20.14	2.76	0.92	0.94	CNKR
34.707	41.022	−11.43	1.98	0.83	0.92	OSMC
34.422	41.150	−7.40	−2.56	1.80	2.26	KRGI
34.379	40.155	−21.40	3.83	0.70	0.67	SNGR
34.780	40.888	−15.10	4.43	0.83	0.93	DDRG
34.814	40.145	−19.54	3.75	0.93	1.03	ALA1
35.113	40.949	−13.70	6.22	1.04	1.15	GHAC
35.054	40.802	−14.66	5.05	0.86	0.96	HMMZ
35.316	40.666	−15.36	5.75	1.02	1.19	GKCB
35.166	41.146	−7.80	4.97	1.01	1.20	GOL1
35.830	40.681	−13.95	7.53	0.91	1.02	GBAG
35.645	40.919	−11.12	7.28	0.99	1.12	HVZA
35.604	40.471	−20.26	2.84	1.03	1.18	GYNC
36.046	41.065	−3.59	4.87	1.10	1.29	KVAK

In the table, long – longitude of the sites, lat – latitude of the sites, E Vel – east velocity component, N Vel – north velocity component, E σ – east velocity error (1 sigma), and N σ – north velocity error (1 sigma).

(Şengör and Kidd, 1979; Şengör et al., 1985; McClusky et al., 2000; Reilinger et al., 2006). In this study, the GPS velocity field along the central branch of the NAF has been determined and modeled using DEF-NODE software (McCaffrey, 2002). The software can calculate slip partitioning within tectonic blocks using spherical Euler poles to describe both the kinematics of block motions and the slip on the block-bounding faults. Backslip can be applied to estimate the contribution of fault locking to the total velocity field.

The software uses the input parameters such as slip rates of GPS sites, locking depth, the location and geometry of the faults and the dip of faults and seismologic data. The locations of the faults were determined based on morphology, seismicity, mapped faults and historical earthquakes. We had to simplify and generalize the faults in the region. Initially, we set a model with 4 blocks using the main branch of the NAF, Laçin and Sungurlu faults (Fig. 1). However, the Laçin fault (Kaymakçı et al., 2001) was later removed since the model did not resolve any significant slip or rotation along this fault. The faults in all the models were taken as vertical since the best fit is obtained with vertical faults. Testing the locking depth for values raging between 2 and 30 km shows also that the best fit can be obtained with a locking depth of 16 km (Fig. 3).

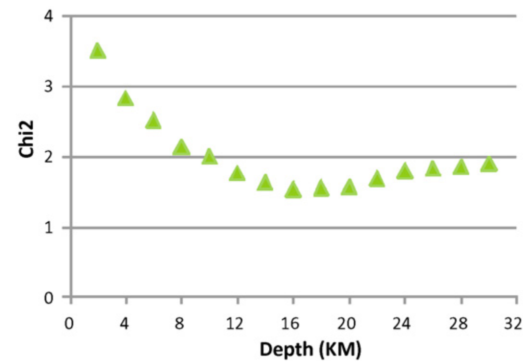

Fig. 3. Plot of reduced χ^2 relative to the assumed depth of the main branch of the NAF. The best fit can be obtained with 16 km locking depth.

The GPS velocity across the faults is well explained by the arctangent function given in Savage and Burford (1973). Figs. 2 and 4 illustrate the elastic strain accumulation revealed by the GPS measurements and the model. The profiles are affected by two faults

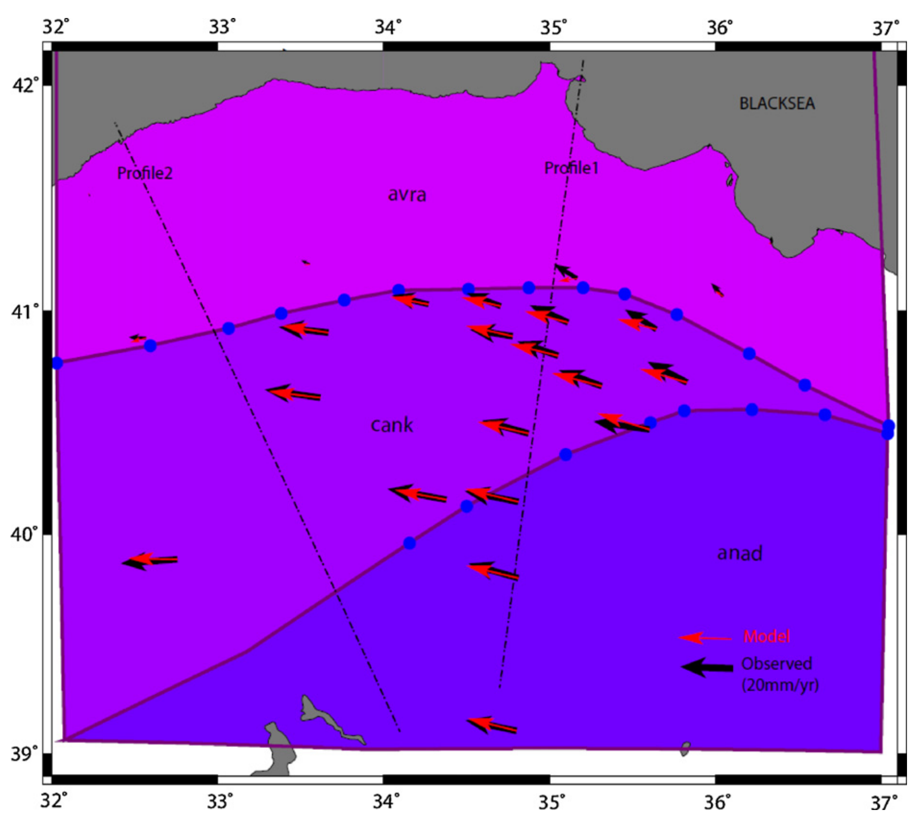

Fig. 2. The observed (black) and modeled (red) GPS velocities relative to Eurasia fixed in ITRF2000. The GPS vectors are modeled using block rotation and back slip on the main branch of the NAF and Sungurlu fault using DEF-NODE (McCaffrey, 2002); anad is the Anatolian block, avra is the Eurasian block, and cank is the interior block delaminated by local faults shown in Fig. 1. The dashed line shows the profile locations across the faults. (For interpretation of the references to color in this figure legend, the reader is referred to the web version of this article.)

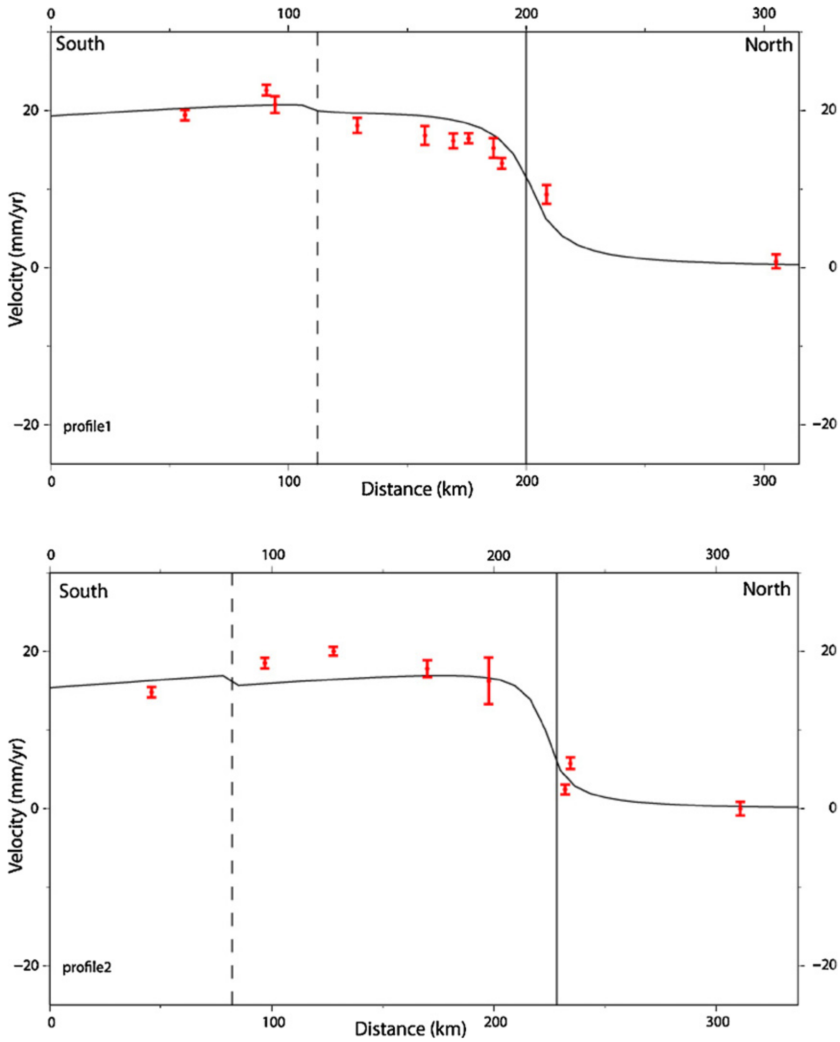

Fig. 4. Profiles showing the GPS velocities (with vertical error bars) approximately perpendicular to the main branch of the NAF and Sungurlu fault as illustrated with dashed line in Fig. 2. The solid line represents the main branch and dashed line shows the Sungurlu fault in these figures. The bold red lines indicate the plate velocity. (For interpretation of the references to color in this figure legend, the reader is referred to the web version of this article.)

extended in the region that are the main branch of the NAF and Sungurlu fault.

4. Slip rate

The geological slip rate of the NAF reported in the literature ranges from 20.5 ± 5.5 to 27 ± 7 mm/yr (Kozacı et al., 2007; Hartleb et al., 2003; Hubert-Ferrari et al., 2002). It is difficult to compare the present-day rates of faulting and the long-term geological rates because of the large uncertainties on most of the geological estimates (Reilinger et al., 2006). However, the reported geological slip rate gives a good coherence as compare well with the GPS-derived slip rates (Fig. 2).

The GPS-derived slip rate of the MID-NAF acquired from this study ranges from 18.7 ± 1.6 to 21.5 ± 2.1 mm/yr on the main branch of the NAF as shown in Fig. 2. On the Sungurlu fault, it has a small slip rate compared to the main branch.

5. Discussion and conclusion

Our GPS measurements along the central part of the NAF show that the average slip rate of the main branch is 20.5 ± 1.8 mm/yr consistent with results obtained by McClusky et al. (2000) and Reilinger et al. (2006). In the study area described in Fig. 1, there are many small continental blocks delimited by the NAF and its splays. In the southern part of the NAF in the study region, a significant slip rate has not been determined along the Sungurlu fault. This could well be due to a deep locking depth (no meaningful velocity gradient), or the result of slip partitioning along the secondary faults to the south of the main branch and the small deformation along each fault. In the light of the geometry of the faults, the second interpretation supports the kinematics of the southern block.

The region between the Sungurlu fault and main branch of the NAF is divided into several blocks by different splays and branches of the NAF. Palaeomagnetic data indicate that each of these fault-bounded blocks was affected by different degrees of block rotation (Tatar et al., 1995; Piper et al., 1997; İşseven and Tüysüz, 2006). ∼20° anticlockwise rotation by Piper et al. (1997) and 30–40° anticlockwise and clockwise rotations by Tatar et al. (1995) have been reported. İşseven and Tüysüz (2006) concluded that the fault-bounded blocks rotated around a vertical axis clockwise and anticlockwise up to 30°. Differences in the azimuth of the residual velocity vectors in the Anatolian collage can be attributed to ongoing slow rotation. Although residual velocities show dominant movement towards the west as expected, some blocks, such as Osmancık and Gümüşhacıköy (Fig. 1), diverge from east–west direction and this can be attributed to ongoing rotation.

As most of the block-bounding faults follow lithological contacts and older tectonic structures such as thrust systems, it can be concluded that our GPS results support the idea of Şengör et al. (2004) that the palaeotectonic structure of the continental crust controls the geometry and behavior of the active faults. But, the ongoing deformation accumulation produces important questions about the secondary systems for the potential earthquake hazard. Our results show that the main part of the slip rate (90 ± 5%) is on the NAF while offshoots share the remaining part (10 ± 5%) of the slip rate.

Acknowledgements

This study is a result of the project entitled "*Determination of kinematics along the North Anatolian Fault and its branches between Ladik and Ilgaz with GPS measurements*" and funded by the Scientific and Technical Research Council of Turkey (TUBITAK) and Istanbul Technical University (ITU) with project numbers 101Y035 and 1636, respectively. We would like to thank all the participants in GPS measurements who helped during the fieldwork to make campaigns successful. We thank Bob King and Tom Herring for GAMIT analysis support and Afyon Kocatepe University and Geomatics Company for the equipment supports. Special thanks to Hamamözü, Osmancık and Alaca Municipalities for their logistic supports. The maps in this paper were produced using the public domain Generic Mapping Tools (GMT) software (Wessel and Smith, 1995)

References

Ambraseys, N.N., Finkel, C.F., 1995. The Seismicity of Turkey and Adjacent Areas: A Historical Review, 1500–1800. Muhittin Salih EREN, Istanbul, Turkey, 240 pp.

Avşar, U., İşseven, T., 2009. Regional clockwise rotation of the Armutlu Peninsula, Western Turkey, resolved from palaeomagnetic study of Eocene volcanic. Tectonophysics 475, 415–422.

Barka, A.A., 1992. The North Anatolian Fault zone. Annales Tectonicae (Special Issue) 6, 164–195.

Barka, A.A., 1996. Slip distribution along the North Anatolian Fault associated with the large earthquakes of the period 1939–1967. Bulletin of Seismic Society of America 86, 1238–1254.

Eyidoğan, H., Güçlü, U., Utku, Z., Değirmenci, E., 1991. Macroseismic Guide of Turkey's Large Earthquakes (1900–1988). İTÜ, Faculty of Mines, Geophysics Department Publication, 198 pp. (in Turkish).

Hartleb, R.D., Dolan, J.F., Akyüz, H.S., Yerli, B., 2003. A 2000 year-long paleoseismologic record of earthquakes along the central North Anatolian Fault, from trenches at Alayurt, Turkey. Seismological Society of America Bulletin 93, 1935–1954.

Hubert-Ferrari, A., Armijo, R., King, G., Meyer, B., Barka, A.A., 2002. Morphology, displacement, and slip rates along the North Anatolian Fault, Turkey. Journal of Geophysical Research 107 (B10), 9/1–9/33.

İşseven, T., Tüysüz, O., 2006. Paleomagnetically defined rotations of fault-bounded continental blocks in the North Anatolian Shear Zone, North Central Anatolia. Journal of Asian Earth Sciences 28, 469–479.

Kaymakçı, N., Özçelik, Y., White, S.H., Van Dijk, P.M., 2001. Neogene tectonic development of the Çankırı basin (central Anatolia, Türkiye). Türkiye Petrol Jeologları Derneği Bülteni 13, 27–56.

Kaymakçı, N., Duermeijer, C.E., Langereis, C., White, S.H., van Dijk, P.M., 2003. Oroclinal bending due to indentation: a paleomagnetic study for the early Tertiary evolution of the Çankırı Basin (central Anatolia, Turkey). Geological Magazine 140 (3), 343–355.

Kaymakçı, N., Aldanmaz, E., Langereis, C., Spell, T.L., Gurer, O.F., Zanetti, K.A., 2007. Late Miocene transcurrent tectonics in NW Turkey: evidence from palaeomagnetism and ^{40}Ar–^{39}Ar dating of alkaline volcanic rocks. Geological Magazine 144 (2), 379–392.

King, R.W., Bock, Y., 2003. Documentation for the GAMIT GPS Analysis Software, Release 10.1. Massachusetts Institute of Technology, Cambridge, MA, USA.

Kozacı, O., Dolan, J.F., Finkel, R., Hartleb, R., 2007. Late Holocene slip rate for the North Anatolian Fault, Turkey, from cosmogenic ^{36}Cl geochronology: Implications for the constancy of fault loading and strain release rates. Geology 35, 867–870.

McCaffrey, R., 2002. Crustal block rotations and plate coupling, in Plate Boundary Zones. Geodynamics Series 30, 101–122.

McClusky, S., Balassanian, S., Barka, A., Demir, C., Ergintav, S., Georgiev, I., Gurkan, O., Hamburger, M., Hurst, K., Kahle, H., Kastens, K., Kekelidze, G., King, R., Kotzev, V., Lenk, O., Mahmoud, S., Mishin, A., Nadriya, M., Ouzounis, A., Paradissis, D., Peter, Y., Prilepin, M., Reilinger, R., Şanlı, I., Seeger, H., Tealeb, A., Toksöz, M.N., Veis, G., 2000. Global Positioning System constraints on plate kinematics and dynamics in the eastern Mediterranean. Journal of Geophysical Research 105, 5695–5719.

Okay, A.I., Tüysüz, O., 1999. Tethyan sutures of Northern Turkey. Geological Society of London, Special Issue 156, 475–515, doi:10.1144/GSL.SP.1999.156.01.22.

Piper, J.D.A., Moore, J.M., Tatar, O., Gürsoy, H., Park, R.G., 1996. Palaeomagnetic study of crustal deformation across an intracontinental transform: the North Anatolian Fault zone in northern Turkey. Geological Society Special Publication 105, 299–310.

Piper, J.D.A., Tatar, O., Gürsoy, H., 1997. Deformational behavior of continental lithosphere deduced from block rotations across the North Anatolian Fault zone in Turkey. Earth and Planetary Science Letters 150, 191–203.

Platzman, E.S., Platt, J.P., Tapırdamaz, M.C., Sanver, M., Rundle, C.C., 1994. Why are there no clockwise rotations along the North Anatolian Fault Zone? Journal of Geophysical Research 99, 21705–21715.

Platzman, E.S., Tapırdamaz, C., Sanver, M., 1998. Neogene anticlockwise rotation of central Anatolia (Turkey): preliminary palaeomagnetic and geochronological results. Tectonophysics 299, 175–189.

Reilinger, R., McClusky, S., Vernant, P., Lawrence, S., Ergintav, S., Çakmak, R., Özener, H., Kadirov, F., Guliev, I., Stepanyan, R., Nadariya, M., Hahubia, G., Mahmoud, S., Sakr, K., ArRajehi, A., Paradissis, D., Al-Aydrus, A., Prilepin, M., Guseva, T., Evren, E., Dmitrotsa, A., Filikov, S.V., Gomez, F., Al-Ghazzi, R., Karam, G., 2006. GPS constraints on continental deformation in the Africa–Arabia, Eurasia continental collision zone and implications for the dynamics of plate interactions. Journal of Geophysical Research—Solid Earth 111, B05411.

Savage, J., Burford, R., 1973. Geodetic determination of relative plate motion in central California. Journal of Geophysical Research 78, 832–845.

Şengör, A.M.C., Kidd, W.S.F., 1979. Post-collisional tectonics of the Turkish–Iranian plateau and a comparison with Tibet. Tectonophysics 55, 361–376.

Şengör, A.M.C., Yılmaz, Y., 1981. Tethyan evolution of Turkey: a plate tectonic approach. Tectonophysics 75, 181–241.

Şengör, A.M.C., Görür, N., ve Şaroğlu, F., 1985. Strike-slip faulting and related basin formation in zones of tectonic escape: Turkey as a case study. Society of Economic Paleontologists and Mineralogists Special Publications 37, 227–264.

Şengör, A.M.C., Tüysüz, O., İmren, C., Sakınç, M., Eyidoğan, H., Görür, N., Le Pichon, X., Rangin, C.C., 2004. The North Anatolian Fault: a new look. Annual of Review of Earth and Planetary Sciences 33, 1–75.

Tari, E., King, R.W., 2002. An experiment on the parameterization of atmospheric estimates by Global Positioning System. In: Proceedings of International Symposium on Geographic Information Systems, September, 23–26, Istanbul, Turkey, pp. 582–591.

Tatar, O., Piper, J.D.A., Park, R.G., Gürsoy, H., 1995. Paleomagnetic study of block rotations in the Niksar overlap region of the North Anatolian Fault Zone, central Turkey. Tectonophysics 244, 251–266.

Tatar, O., Piper, J.D.A., Gürsoy, H., Temiz, H., 1996. Regional significance of Neotectonic counterclockwise rotation in central Turkey. International Geology Review 38, 692–700.

Wessel, P., Smith, W.H.F., 1995. New version of the generic mapping tools released. EOS Transactions—American Geophysical Union 76, 329.